Plasma wakefield acceleration at CLARA facility in Daresbury Laboratory

G. Xia[a,b], Y. Nie[c], O. Mete[a,b], K. Hanahoe[a,b], M. Dover[a], M. Wigram[a], J. Wright[a], J. Zhang[a], J. Smith[d], T. Pacey[a,b], Y. Li[a,b], Y. Wei[b,e], C. Welsch[b,e]

[a]*School of Physics and Astronomy, University of Manchester, Manchester, United Kingdom*
[b]*The Cockcroft Institute, Sci-Tech Daresbury, Daresbury, Warrington, United Kingdom*
[c]*Deutsche Elektronen-Synchrotron DESY, Hamburg, Germany*
[d]*Tech-X UK Corporation, Daresbury Innovation Centre, Warrington, United Kingdom*
[e]*University of Liverpool, Liverpool, United Kingdom, United Kingdom*

Abstract

A plasma accelerator research station (PARS) has been proposed to study the key issues in electron driven plasma wakefield acceleration at CLARA facility in Daresbury Laboratory. In this paper, the quasi-nonlinear regime of beam driven plasma wakefield acceleration is analysed. The wakefield excited by various CLARA beam settings are simulated by using a 2D particle-in-cell (PIC) code. For a single drive beam, an accelerating gradient up to 3 GV/m can be achieved. For a two bunch acceleration scenario, simulation shows that a witness bunch can achieve a significant energy gain in a 10-50 cm long plasma cell.

Keywords: Plasma wakefield acceleration, Particle-in-cell, Quasi-nonlinear regime, Two-bunch acceleration

1. Introduction

Plasma wakefield acceleration is one of the most promising technologies to miniaturize the scale of next generation particle accelerators due to its capability to sustain very large electric field. From the initial idea proposed to nowadays, plasma based accelerators have achieved tremendous breakthroughs in the last three decades [1, 2]. Plasma accelerators driven by high power and short pulse lasers, so-called laser wakefield acceleration (LWFA) could achieve hundreds MeV to several GeV electron beam in a single stage acceleration. The resultant monoenergetic beams have the energy spread of only a few percent [3, 4, 5]. The recent highlight from LBNL has successfully demonstrated a 4.25 GeV electron beam acceleration from a 9 cm long capillary discharge plasma source [6]. This electron beam energy is already well comparable to most of today's third generation light sources and the resulting beam can be used to drive free electron laser as well [7] . On the other hand, the plasma accelerators driven by electron beam, so-called beam driven plasma wakefield acceleration (or PWFA) has doubled the energy of the electron beam from the Stanford Linear Collider (SLC) within an 85 cm plasma cell [8]. The FACET facility has recently also achieved the high efficient acceleration for a separate witness electron bunch [9]. The latest results showed that positron beam can also excite significant wakefield and accelerate the positrons at the rear part of the bunch in a self-loaded mode [10]. All these breakthroughs have shown great promise to build tabletop and efficient energy use of plasma accelerators as alternatives to conventional accelerators. This is mainly due to plasma based accelerators can provide an accelerating gradient of 1-100 GeV/m, which are usually over two to three orders of magnitude higher than the field in conventional RF-based accelerating structures (in general equal or less than 100 MeV/m) [11].

Compared to laser driven wakefield accelerators, the advantages of a relativistic beam driven plasma wakefield acceleration lie in that the beam can propagate in plasma for much longer distances than that of the laser beam in plasma, as the laser beam is subject to the 3D effect, i.e. diffraction, depletion and dephasing in the plasma. Therefore the energy gain for a one-stage acceleration is significant for PWFA. Secondly, the conventional RF-based accelerator can obtain the relativistic electron beam with relatively high efficiency (usually more than 10%). Using this relativistic beam as drive beam for plasma wakefield excitation is more efficient than using the laser beam for beam acceleration (if compared to low wall-plug efficiency for producing laser beam). Currently, there are a number of dedicated facilites to demonstrate the great potential of the beam driven plasma wakefield acceleration method, e.g. FACET and FACET II facility at SLAC[12] , the FLASHForward at DESY[13], the SPARC LAB facility of INFN[14] and the AWAKE experiment driven by the 400 GeV proton beam from the SPS at CERN[15, 16, 17, 18], etc.

We have proposed a high gradient plasma wakefield acceleration experiment based at CLARA (Compact Linear Advanced Research Accelerator) facility in the Daresbury Laboratory[19, 20, 21]. The idea is to investigate the critical issues for the next generation plasma accelerators, e.g. test of the PWFA theory, high acceleration gradient (1-10 GeV/m), two-bunch acceleration, high transformer ratio, plasma focusing effect (plasma lens), and related advanced beam dynamics concepts etc. Since the CLARA beam is designed for Free Electron Laser (FEL) research, which makes the beam ideal for plasma wakefield acceleration experiments. Firstly, the beam is relativistic so it can propagate in plasma for a long distance, i.e. tens of centimetres. Therefore the energy gain from a one-stage acceleration will be

significant. Secondly, the bunch length can be tuned from a few pico-second down to tens of femtosecond, which enables us to study the scaling laws for PWFA and reach high accelerating gradient in an ultrashort bunch operation case. Thirdly, the well-developed beam diagnostics at CLARA can be easily employed to characterise beam precisely, and knowing the beam parameters are crucial for PWFA experiments.

In this paper, the theory of quasi-nonlinear PWFA regime (QNL) is introduced and analysed in section 2. The particle-in-cell (PIC) code VSIM [22] is employed to model the electron-plasma interactions for a single drive beam and two bunch acceleration case respectively based on the CLARA beam parameters. The detailed simulation results are presented in section 3.

2. PWFA in quasi-nonlinear regime

In the blowout regime of PWFA, the driving bunch has much higher electron density n_b than the background plasma density n_p, i.e. $n_b >> n_p$, and thus excites an ion filled bubble behind it. The radial focusing field is linear along the bubble radius and the longitudinal accelerating field is constant in radius. However, the nonlinear plasma oscillation occurs simultaneously, which limits the beam quality of the witness bunches. Therefore, a new regime called weak blowout has been proposed and investigated recently [23, 24, 25]. It operates in the quasi-nonlinear regime (QNL), where the total charge of the driving bunch is relatively low to maintain the resonant plasma response, especially a constant wakefield frequency, while the density of the driving bunch is still larger than that of the plasma to form the bubble. Such a driving bunch can be achieved by using a cigar shape, where the transverse size of the bunch σ_r is much smaller than the bunch length σ_z, i.e. $\sigma_r << \sigma_z$. The QNL-PWFA is very promising to provide high-quality and high-energy bunches under ultra-high accelerating gradient. Meanwhile, the transformer ratio is also an important figure of merit, which is defined as the ratio of the maximum accelerating wakefield behind the driving bunch and the maximum decelerating wakefield within it, i.e. $R = W_{acc}/W_{dec}$. R is usually less than two for a single symmetric driving bunch in the linear regime. Fortunately, there are a few ways to overcome this limit, for instance, using an asymmetric driving bunch [26, 27], a ramped bunch train [28, 29] and the nonlinear plasma dynamics [27, 30] as in the case of single bunch driven QNL-PWFA.

In the QNL-PWFA regime, several case studies have been performed by using 2D particle-in-cell simulations. The idea is to find out the optimal plasma density for certain driving beam parameters. In order to enhance the transformer ratio, one can manipulate the driving bunch shape, namely the ratio of σ_r to σ_z. The test bunches to be used are typically achievable at a few existing and oncoming facilities at the energy level of hundreds of MeV, e.g. at CLARA facility. The driving bunches have the azimuthally symmetric bi-Gaussian shape as follows:

$$n_b(r, z) = n_b e^{-r^2/2\sigma_r^2} e^{-z^2/2\sigma_z^2}, \tag{1}$$

here n_b is the driving beam density which is given by

$$n_b = N_b/((2\pi)^{3/2}\sigma_r^2\sigma_z), \tag{2}$$

The normalized charge that is used to evaluate the nonlinearity in the PWFA is defined as the total electron numbers in the driving bunch N_b normalized to the numbers of the plasma electrons inside a cubic plasma skin depth k_p^{-3} as follows [23]

$$\tilde{Q}_n = N_b k_p^3/n_p = n_b/n_p(2\pi)^{3/2}k_p\sigma_z(k_p\sigma_r)^2, \tag{3}$$

where $k_p = 2\pi/\lambda_p = \sqrt{e^2 n_p/m_e\epsilon_0}/c$ is the plasma wave number with λ_p the plasma wavelength. In linear theory, the number of the plasma electrons that response to the driving beam is approximately limited to $n_p k_p^{-3}$. It can be seen that $\tilde{Q}_n$ should be smaller than 1 to have linear plasma response. On the other hand, n_b should be higher than (or comparable to) n_p to excite bubbles in plasma. $\tilde{Q}_n < 1$ and $n_b > n_p$ are the two conditions to achieve the QNL-PWFA. It has been demonstrated that the prediction from the linear theory that the maximum accelerating gradient appears at $k_p\sigma_z = \sqrt{2}$ still holds even though the nonlinear blowout regime is reached, i.e. when $n_b >> n_p$, as long as the normalised charge per unit length of the driving beam $\Lambda = (n_b/n_p)(k_p^2\sigma_r^2) \ll 1$ [31]. Therefore, the bunch with a cigar shape ($\sigma_r \ll \sigma_z$) is the best candidate to drive a PWFA in the QNL regime.

For the QNL-PWFA, the maximum accelerating wakefield may be estimated by the following equation of the linear theory:

$$E_{z,max} \approx 236MV/m(\frac{N_b}{4 \times 10^{10}})(\frac{600}{\sigma_z(\mu m)})^2 \ln(\sqrt{\frac{10^{16}}{n_p(cm^{-3})}}\frac{50}{\sigma_r(\mu m)}), \tag{4}$$

which shows that $E_{z,max}$ depends not only on the driving bunch charge and length, but also on the optimum plasma density and the bunch spot size σ_r. According to the linear theory, the optimal plasma density occurs at $k_p\sigma_z = \sqrt{2}$. However, beyond this limit $\sigma_r \ll \sigma_z$ when σ_r approaching σ_z, the optimal plasma density n_p will be lower and $k_p\sigma_z < \sqrt{2}$ [32], since in this case the driving bunch density n_b will be likely decreases along with the increasing of the spot size. In addition, $E_{z,max}$ can also be predicted by the following expression if $n_b/n_p \leq 10$ [32]:

$$E_{z,max}/E_{0,max} \approx 1.3(n_b/n_p)(k_p\sigma_r)^2 \ln(1/k_p\sigma_r), \tag{5}$$

for the narrow driving bunch, i.e. $k_p\sigma_r < 0.3$ and in the weakly nonlinear limit $\Lambda < 1$, where the wave breaking wakefield $E_{0,max} = mc\omega_p/e \sim 100\sqrt{n_p(cm^{-3})}$ V/m.

The maximum energy that can be given to the witness bunch is limited by the transformer ratio R. For the single symmetric driving bunch, the limit of $R < 2$ can be overcome by operating the PWFA in the QNL regime, where nonlinear blowout occurs. It is meaningful to study the dependence of R on the plasma density for given driving bunch parameters. Due to the incomplete nonlinear theories, numerical simulations must be employed to study the detailed wakefield structures in the QNL regime.

3. Simulation study of beam-plasma interactions

3.1. Electron beam from CLARA facility

CLARA is a normal conducting linear electron accelerator. It can generate ultrashort and bright electron bunches and use these bunches in the experimental production of stable, synchronised, ultrashort photon pulses of coherent light from a single pass free electron laser (FEL) with techniques directly applicable to the future generation of light source facilities [19]. The CLARA facility comprises of a photo-injector electron gun, S-band normal conducting accelerating cavities, magnetic bunch compressor, fourth harmonic lineariser, dedicated beam diagnostic sections at low and high energies and FEL beam line, as illustrated in Fig. 1. CLARA facility can provide 250 MeV electron bunch with bunch charge of 250 pC. The detailed electron beam parameters are listed in Table 1.
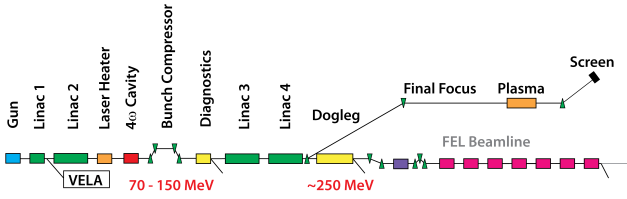

Figure 1: Conceptual layout of the CLARA facility and the PARS beam line.

For the electron beam driven plasma wakefield experiment at PARS (Plasma Accelerator Research Station), a dogleg will be built to guide the CLARA beam to a parallel beam line, offset by $\sim 1.5m$ from the CLARA beam axis, but still contained within the CLARA shielding area. The conceptual layout of the PARS beam line is also shown in Fig. 1. It consists of the dogleg beam line, final focus, plasma cell, energy spectrometer and a final beam dump (not shown). The dogleg beam line consists of arrays of dipoles and quadrupoles to guide and focus the beam from the CLARA beam line to the PARS. The final focus, which is prior to the plasma cell, is designed to focus the electron beam transversely and to match the electron beam parameters with the plasma parameters. A variable length capillary discharge plasma source (10-50 cm) is currently being built at Daresbury Laboratory. The key issues for the PWFA at various beam and plasma parameter ranges will be studied extensively, including the PWFA in QNL regime An energy spectrometer will be employed to characterise the energy of electrons exiting the plasma cell. The final beam dump will absorb the energy of electrons after exiting the plasma cell. Prior to the final focus and plasma cell, a magnetic chicane may be needed to compress the bunch further to an extremely short length.

3.2. Wakefield optimisation for one drive bunch in QNL regime

2D particle-in-cell simulations have been performed using the software VSim from the Tech-X Corporation [22]. The first relativistic driving bunch has the following parameters $N_b = 1.56 \times 10^9$ (bunch charge of 250 pC), $\sigma_z = 75\mu m$, $\sigma_r = 20\mu m$ and $n_b = 3.31 \times 10^{15} cm^{-3}$. For the above parameters, $\Lambda = 0.048$ and the optimum plasma density for the maximum accelerating gradient is $9.8 \times 10^{15} cm^{-3}$ according to the linear theory. The plasma density scanned is thus from $3.3 \times 10^{14} cm^{-3}$ to $3.3 \times 10^{16} cm^{-3}$ so as to cover all interested ranges.

When $n_p \leq 8 \times 10^{15} cm^{-3}$ we have $\tilde{Q}_n < 1$ and $n_b > n_p$ (or $n_b \approx n_p$), so the PWFA will work in the QNL regime. For the cases of $n_p > 8 \times 10^{15} cm^{-3}$, $\tilde{Q}_n > 1$ and $n_b \ll n_p$, thus the linear response occurs. Over the studied plasma range, the parameters $k_p\sigma_r$ and $k_p\sigma_z$ vary from 0.07 to 0.69 and 0.26 to 2.59, respectively. The dependences of the decelerating wakefield W_{dec}, the accelerating wakefield W_{acc} and the transformer ratio R on the plasma density n_p are shown in Fig.2. At the lower plasma densities, $k_p\sigma_z \ll 1$, i.e. the driving bunch is much shorter than a plasma skin depth. As a result, the blowout will occur and the wakefield will depend on the total charge of the bunch other than the peak current. From Eq. (3) we can see that the normalized total charge $\tilde{Q}_n \propto \sqrt{n_p}$. This is why both of W_{dec} and W_{acc} increase as n_p increases at the beginning in Fig.2. In the intermediate plasma density range, as $k_p\sigma_z$ increases, there is an optimum value of $n_p = 6.5 \times 10^{15} cm^{-3}$ that gives the maximum W_{acc} about 2.25 GV/m. Here we have $\tilde{Q}_n = 0.87$, $n_b/n_p = 0.51$ and $k_p\sigma_r = 0.31$. The optimal parameter $k_p\sigma_z = 1.15$ is 0.81 times the prediction from the linear theory ($k_p\sigma_z = \sqrt{2}$ from the linear theory), since the bunch is not ideally narrow with the ratio of $\sigma_r/\sigma_z = 0.27$. Notice that the calculated accelerating wakefields using Eq. (4) and Eq. (5) are 668 MV/m and 594 MV/m, 3.4 and 3.8 times lower than the simulation results, respectively. As n_p increases further, the wakefield becomes weaker and weaker, since the ambient electrons are only perturbed and the driving bunch length becomes longer than the plasma wavelength so the wakefield can only be driven by a part of the bunch unless the self-modulation instability is resonantly excited. As for the transformer ration R, it increases quickly at the beginning and becomes saturated around 2.36 when n_p is about $1.5 \times 10^{16} cm^{-3}$. It is important to figure out that when the accelerating gradient reaches the maximum value of 2.25 GV/m, $R \approx 2.1$ is still much lower than the saturated value. Figures 3 and 4 plot the longitudinal wakefield distribution and the longitudinal accelerating field after the bunch propagates through 29.7 mm in plasma with an optimum plasma density $n_p = 6.5 \times 10^{15} cm^{-3}$ for the first driving bunch, respectively. It can be seen that the PWFA works in the weakly blowout regime, and the bubble radius can be roughly estimated as twice the equilibrium channel radius $R_b \approx 2\sigma_r\sqrt{n_b/n_p} = 2\sqrt{\Lambda}/k_p$ [33], which is $29\mu m$. The value of $k_p R_b \approx 0.44 < 1$, so the wakefield structure is dominated by the linear plasma response, as shown in Fig. 4.

In order to improve the wakefield gradient as well as the transformer ratio, we decrease the ratio of σ_r/σ_z while keeping the total electron charge unchanged. The second driving bunch parameters are as follows: $N_b = 1.56 \times 10^9$, $\sigma_z = 100\mu m$, $\sigma_r = 10\mu m$ and $n_b = 9.92 \times 10^{15} cm^{-3}$ that has been enhanced. The smaller transverse size of the bunch may be obtained by using a triplet of permanent magnet quadrupoles as used in the Accelerator Test Facility (ATF) at BNL. For the above parameters, $\Lambda = 0.036$ and the optimum n_p to have the maximum accelerating gradient is $5.5 \times 10^{15} cm^{-3}$ according to the linear theory. We used the same n_p range as in the first case. The ma-

Table 1: Three operation regimes for the PWFA experiment at the CLARA/PARS facility.

Operating modes	Long Pulse	Short Pulse	Ultra-Short Pulse
Beam energy (GeV)	250	250	250
Charge/Bunch Q (pC)	250	250	20-100
Electron/Bunch N_b ($\times 10^9$)	1.56	1.56	0.125-0.625
Bunch length rms (fs)	250-800	100-250	≤ 30
Bunch length (μm)	75-240	30-75	9
Bunch radius (μm)	10-100	10-100	10-100
Normalised emittance (mm mrad)	≤ 1	≤ 1	≤ 1
Energy spread (%)	1	1	1

jority points locate at $\tilde{Q}_n < 1$ and $n_b > n_p$, while $k_p\sigma_r$ and $k_p\sigma_z$ varying from 0.035 to 0.35 and 0.35 to 3.5, respectively. Figure 5 shows that the optimum n_p is near $5 \times 10^{15} cm^{-3}$, where $\tilde{Q}_n = 0.76$, $n_b/n_p = 2.0$ and $k_p\sigma_r = 0.13$. The parameter $k_p\sigma_z = 1.35$ becomes much closer to $k_p\sigma_z = \sqrt{2}$ compared to the previous case, since the ratio of σ_r/σ_z has been reduced to 0.1 and the bunch is narrower than before. Figure 6 plots the longitudinal wakefield distribution at the optimum plasma density of $5 \times 10^{15} cm^{-3}$ after the bunch traveling in a 31.5 mm plasma. It can be seen that the wakefield in first accelerating bubble is very strong. The details can also be found in Fig.7, the maximum accelerating gradient is $W_{acc} = 3.73 GV/m$, 5.7 and 5.6 times larger than the results from Eq. (4) and Eq. (5), respectively, and $R = 2.3$ is very close to the peak value shown in Fig. 5. In principle, it is possible to merge the two peaks of the accelerating wakefield and the transformer ratio by manipulating the driving bunch shapes. In Fig. 6, it can be seen that the bubble structure is quite clean with a radius of $R_b \approx 40\mu m$ that is greater than the estimation of 28 μm. Compared to the first case study, the optimal plasma wavelength increases from $409\mu m$ to $467\mu m$, and there is no sharp spike in the accelerating wakefield structure, leading to high useful accelerating field [23]. Meanwhile, longer wavelength of the accelerating wakefield allows longer bunch length of the externally injected witness bunch concerning with the field curvature effect, and brings benefit to maintaining high beam quality during acceleration in the plasma [34].

The normalized amplitudes of the accelerating wakefield for the above two cases are plotted in Fig.8. The peak values do not necessarily appear at the optimum plasma densities that give the maximum W_{acc}. The normalized wakefield amplitudes of the second driving bunch are much higher than those of the first one due to the improved bunch shape, but still less than unity.

3.3. Simulation of two-bunch acceleration

To get the benefit from the plasma wakefield, a two-bunch acceleration needs to be studied [12, 35]. In this scheme, the witness bunch will need to follow behind the drive bunch at a position of the maximum accelerating field. Meanwhile a much lower final energy spread is desired after the witness bunch exiting from the plasma. Theoretically the position of witness bunch should be about $\lambda_p/2$ behind the drive beam, i.e. in terms of the wakefield oscillations, a phase-lag of π behind the drive beam. However, due to finite size and the associated electro-
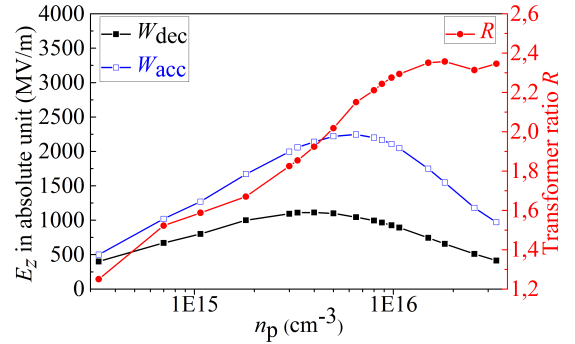

Figure 2: The accelerating/decelerating field and transformer ratio as a function of n_p for the first driving bunch.
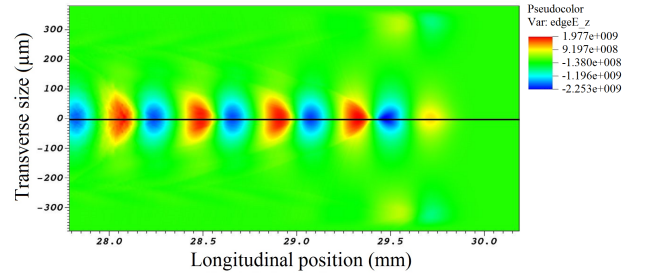

Figure 3: The longitudinal wakefield distribution at the ambient plasma density of $6.5 \times 10^{15} cm^{-3}$ for the first driving bunch.
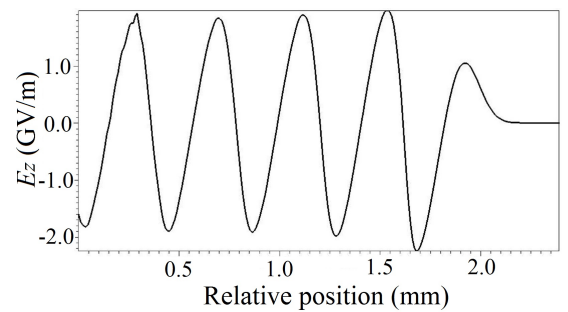

Figure 4: The accelerating wakefield after the bunch propagates through 29.7 mm in plasma for the first driving bunch.

magnetic fields of the electron bunch, the witness beam will distort the shape of the excited wakefield, a phenomenon known as beam loading [36]. This can sometimes alter the wakefield significantly, in both peak position and field magnitude, depending on the strength of the beam loading effect.
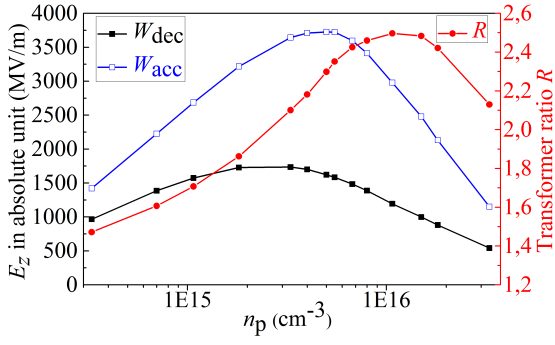
Figure 5: The accelerating/decelerating field and transformer ratio as a function of n_p for strongly focused beam, i.e., the second driving bunch.
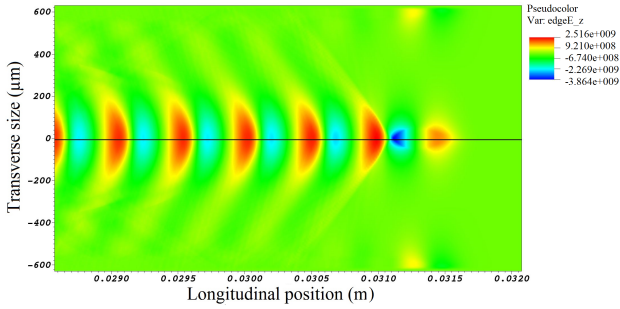

Figure 8: The normalized wakefield amplitudes for different plasma densities using norminal and strong focused driving bunches.

Figure 6: The longitudinal wakefield distribution at the ambient plasma density of $5 \times 10^{15} cm^{-3}$ for the second driving bunch.
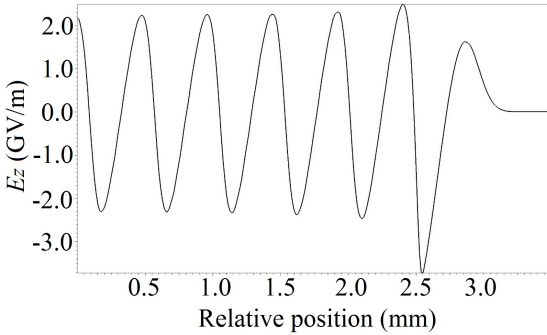

Figure 7: The accelerating wakefield after the bunch propagates through 31.5 mm in plasma, for the second driving bunch.

In order to find an optimum drive-witness phase lag, a two-beam case was implemented for the VSIM simulations. An additional Gaussian beam (witness beam) was introduced to the macro-particle weighting, as shown in Fig. 9, with a beam offset of $\lambda_p/2$ behind the drive beam, plus an additional offset specified by the user. The bunch densities for the drive bunch and witness bunch are shown in Fig. 10. We assume that the witness beam has the same specifications as the drive beam, i.e., its energy, transverse size and bunch length are the same, except an additional weighting factor of 0.2 is introduced so that the witness beam has a bunch charge of 50 pC. An initial energy spread of 1% is also introduced for both the witness and the drive beams, to better match the CLARA beam parameters.

Simulations were performed with the witness beam offset being increased from $0.5\lambda_p$ up to $0.75\lambda_p$ behind the drive
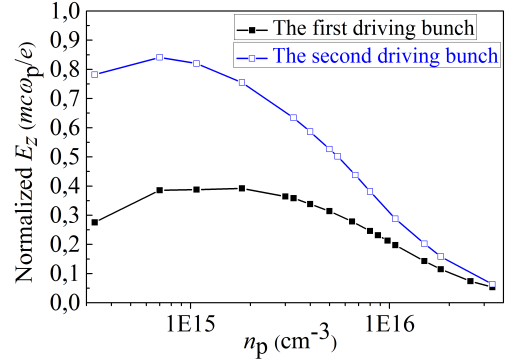
beam for each plasma density of 0.5, 1.0, $3.0 \times 10^{15} cm^{-3}$ and $5.0 \times 10^{15} cm^{-3}$ for a maximum 50 cm long plasma, covering the full potential plasma cell length at PARS. The final average energy of the witness bunch was recorded, and used to calculate an average accelerating gradient experienced by the bunch over the length of the plasma, with the aim of finding the phase-lag that produced the highest average acceleration, and hence the highest final energy.

The resulting average accelerating gradients for the density of $1.0 \times 10^{15} cm^{-3}$ are plotted in Fig.11. The data actually shows the average experienced gradients after 40 cm of propagation in the plasma. After this distance a numerical instability occurs, disrupting the fields and the witness beam energy sharply drops. An identical effect is also observed for the plasma density of $3.0 \times 10^{15} cm^{-3}$, but not for the case when the plasma density is $0.5 \times 10^{15} cm^{-3}$. This is mainly due to the dephasing length for different plasma densities. It is possible that this instability is caused by a breakdown in the physics of the simulation. All the particles in the simulation move at speed of light c, regardless of their energies, so no dephasing occurs and the simulation no longer represents the reality of the laws of the physics. The data after this is considered unreliable and only data acquired up to the instabilities is used.

The maximum average accelerating field experienced is found as $0.8 GV/m$ at an offset of $0.67\lambda_p$, as shown in Fig.11. The beam energy variation for drive bunch and witness bunch as function of propagating distance in plasma is plotted in Fig.12. It can be seen that after a 50 cm long plasma, the drive beam loses its energy and the witness can gain significant amount of energy from the plasma. Figure 13 shows the energy gain and energy loss for a 250 pC, 250 MeV drive bunch with $\sigma_r = 40\mu m$, $\sigma_z = 75\mu m$, and a 50 pC witness bunch with $\sigma_r = 25\mu m$ and $\sigma_z = 10\mu m$ after propagating in a 10 cm long plasma. The distance between the witness bunch to the drive bunch is $\lambda_p/2$, with the witness offset from this by $20\mu m$ forwards. The plasma density is set as an optimum value of $5 \times 10^{21} m^{-3}$ (or $5 \times 10^{15} cm^{-3}$). The lines are linear fits with gradients corresponding to an average decelerating gradient of 289 MeV/m for the drive bunch and an accelerating gradient of 519 MeV/m for the witness. It can be seen that in this case, the energy gain is much more significant than that of the low plasma density case, as shown in Fig.12.
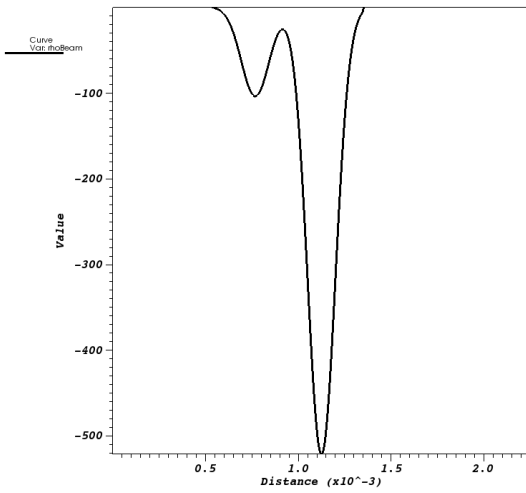
5

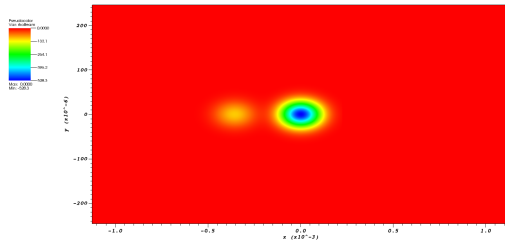Figure 9: Bunch charge for the drive bunch and witness bunch.

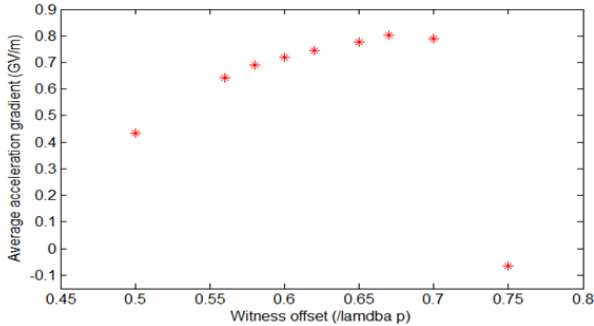Figure 10: Bunch density for the drive bunch and witness bunch.

Figure 11: Average accelerating gradient experienced by the witness beam against witness beam offset behind the drive beam, given as a fraction of λ_p, for a plasma density of $1.0 \times 10^{21} m^{-3}$. The peak in acceleration gradient occurs at $0.67\lambda_p$, with an average gradient of 0.80 GV/m.

4. Conclusions

The PARS facility will be built to study the key issues in the next generation plasma wakefield acceleration based at the CLARA facility at the Daresbury Laboratory. Simulation has shown that the relativistic electron beam from CLARA can excite the plasma wakefield with amplitude up to 3 GV/m in the quasi-nonlinear regime. A witness bunch placed at the appropriate position can gain significant energy in a 10-50 cm long plasma cell with plasma density of $\sim 10^{15}$ cm^{-3}.
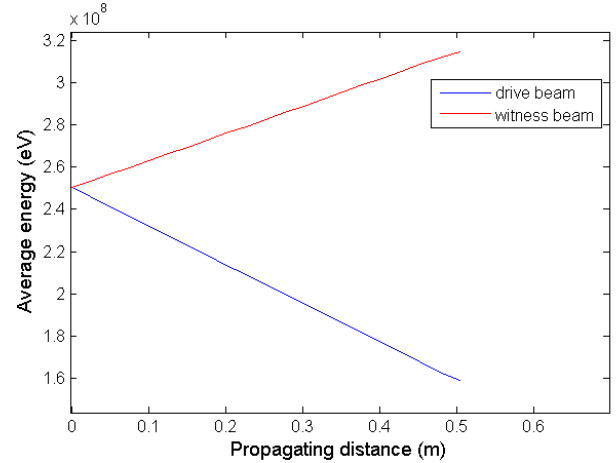

Figure 12: Energy variation for drive bunch and witness bunch as function of propagating distance in plasma with plasma density of $1.0 \times 10^{21} m^{-3}$.
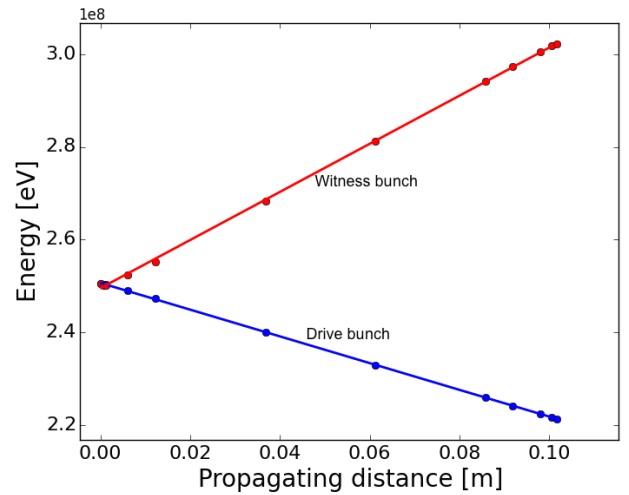

Figure 13: Energy variation for drive bunch and witness bunch as function of propagating distance in plasma with plasma density of $5.0 \times 10^{21} m^{-3}$.

[1] E. Esarey et al., IEEE Transactions on Plasma Science, 24 (1996) 252.
[2] C. Joshi et al., New J. Phys. 12 (2010) 045003.
[3] W. Leemans et al., Nature Physics 2, (2006) 696.
[4] W. Leemans et al., Phys. Today 62 (3) (2009) 44.
[5] X. Wang et al., Nat. Commun. 4 (2013) 2988.
[6] W. Leemans et al., Phys. Rev. Lett. 113, 245002 (2014).
[7] S. Cipiccia et al., Nature Phys. 7 (2011) 867.
[8] I. Blumenfeld et al. Nature 445 (2007) 741.
[9] M. Litos et al. Nature 515 (2014) 92.
[10] S. Corde et al., Nature 524 (2015) 442.
[11] P. Muggli et al., C. R. Physique 10 (2009) 116.
[12] M. J. Hogan et al., New Journal of Phys. 12 (2010) 055030.
[13] J. Grebenyuk et al., Nucl. Instrum. Meth. A 740 (2014) 246.
[14] Andrea R. Rossi et al., Nucl. Instrum. Meth. A 740 (2014) 60.
[15] A. Caldwell et al., CERN-SPSC-2013-013 (2013).
[16] G. Xia et al., AIP Conf. Proc. 1299 (2010) 510.
[17] G. Xia et al., J. Plasma Physics 78 (2012) 347.
[18] R. Assmann et al., Plasma Phys. Control. Fusion 56 (2014) 084013.
[19] J.A. Clarke et al., Journal of Instrumentation 9 (05), (2014) T05001.

[20] G. Xia et al., Nucl. Instrum. Meth. A 740 (2014) 165.

[21] O. Mete et al., Phys. Plasmas 22 (2015) 103117.

[22] http://www.txcorp.com/products/VORPAL/.

[23] J. B. Rosenzweig et al., Phys. Rev. Spec. Topics Acc. Beams 7, (2004) 061302.

[24] J. B. Rosenzweig et al., AIP Conference Proceedings 1507 (2012) 612.

[25] P. Londrillo et al., Nucl. Instrum. Meth. A 740 (2014) 236.

[26] K.L.F. Bane et al., IEEE Trans. Nucl. Sci., NS-32 (1985) 3524.

[27] F. Massimo et al., Nucl. Instrum. Meth. A 740 (2014) 242.

[28] C. Jing et al., Phys. Rev. Lett. 98 (2007) 144801.

[29] B. Jiang et al., Phys. Rev. Spec. Topics Acc. Beams 15, (2012) 011301.

[30] J. B. Rosenzweig et al., Phys. Rev. A 39 (1989) 1586.

[31] W. Lu et al., New Journal of Phys. 12 (2010) 085002.

[32] W. Lu et al., Phys. Plasmas 12 (2005) 063101.

[33] S. Lee et al., Phys. Rev. E 61, (2000) 7014.

[34] J. Grebenyuk et al., Proceedings of IPAC2014 (2014) 1515.

[35] B. Hidding et al., Phys. Rev. Lett 104 (2010) 195002.

[36] N. Vafaei-Najafabadi et al., Phys. Rev. Lett 112 (2014) 025001.